Boosting alkaline water splitting and urea electrolysis kinetic process of Co_3O_4 nanosheet by electronic structure modulation of F, P co-doping

Xiaoqiang Du[a*],Guangyu Ma[a] and Xiaoshuang Zhang[b]

a. School of Chemical Engineering and Technology, North University of China, Taiyuan 030051, People's Republic of China. E-mail: 20160053@nuc.edu.cn

b. School of Science, North University of China, Taiyuan 030051, People's Republic of China.

DFT calculation

The DFT calculations were performed using the Cambridge Sequential Total Energy Package (CASTEP) with the plane-wave pseudo-potential method. The geometrical structures of the (111) plane of F-Co_3O_4, F-P-Co_3O_4, F-S-Co_3O_4 and F-Se-Co_3O_4 were optimized by the generalized gradient approximation (GGA) methods. The Revised Perdew-Burke-Ernzerh of (RPBE) functional was used to treat the electron exchange correlation interactions. A Monkhorst Pack grid k-points of 6*6*1 of F-Co_3O_4, F-P-Co_3O_4, F-S-Co_3O_4 and F-Se-Co_3O_4, a plane-wave basis set cutoff energy of 480 eV were used for integration of the Brillouin zone. The structures were optimized for energy and force convergence set at 0.05 eV/A and 2.0×10^{-5} eV, respectively. The vacuum space was up to 0.002 A to eliminate periodic interactions. the Gibbs free energy of H adsorption was calculated as follows:

$\Delta G_{H^*} = \Delta E_{H^*} + \Delta ZPE - T\Delta S$

Where ΔZPE is the zero-point energy and $T\Delta S$ stands for the entropy corrections. According to the previous report by Norskov et al., we used the 0.24 eV for the ΔZPE - $T\Delta S$ of hydrogen adsorption in this work.

Res: J. Electrochem. Soc., **2005**, 152, J23.

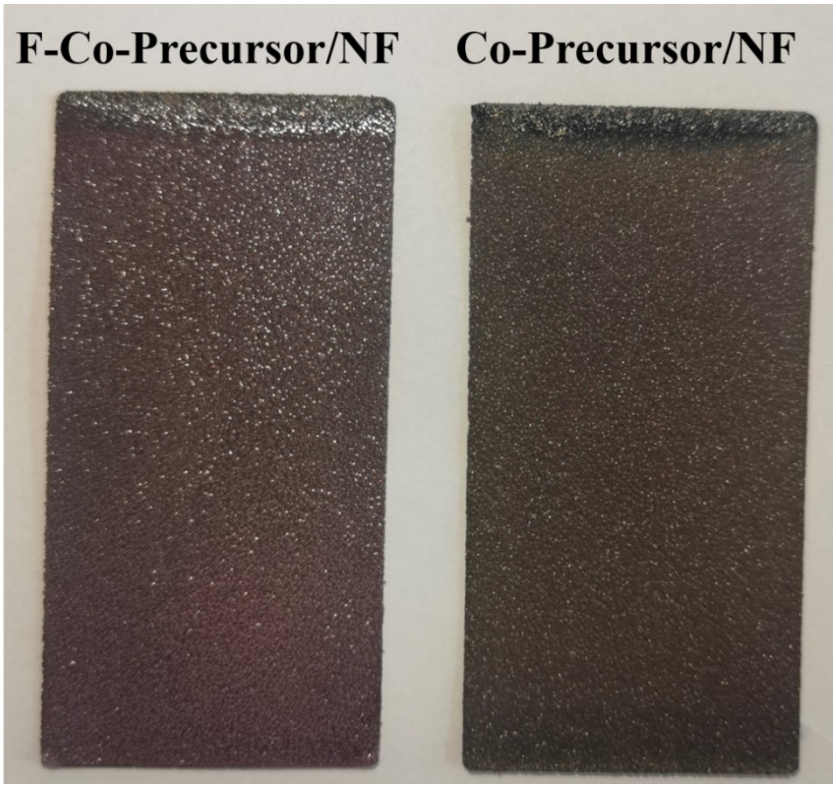

Fig. S1. Electronic images of the synthesized F-Co-precursor /NF and Co-precursor /NF.

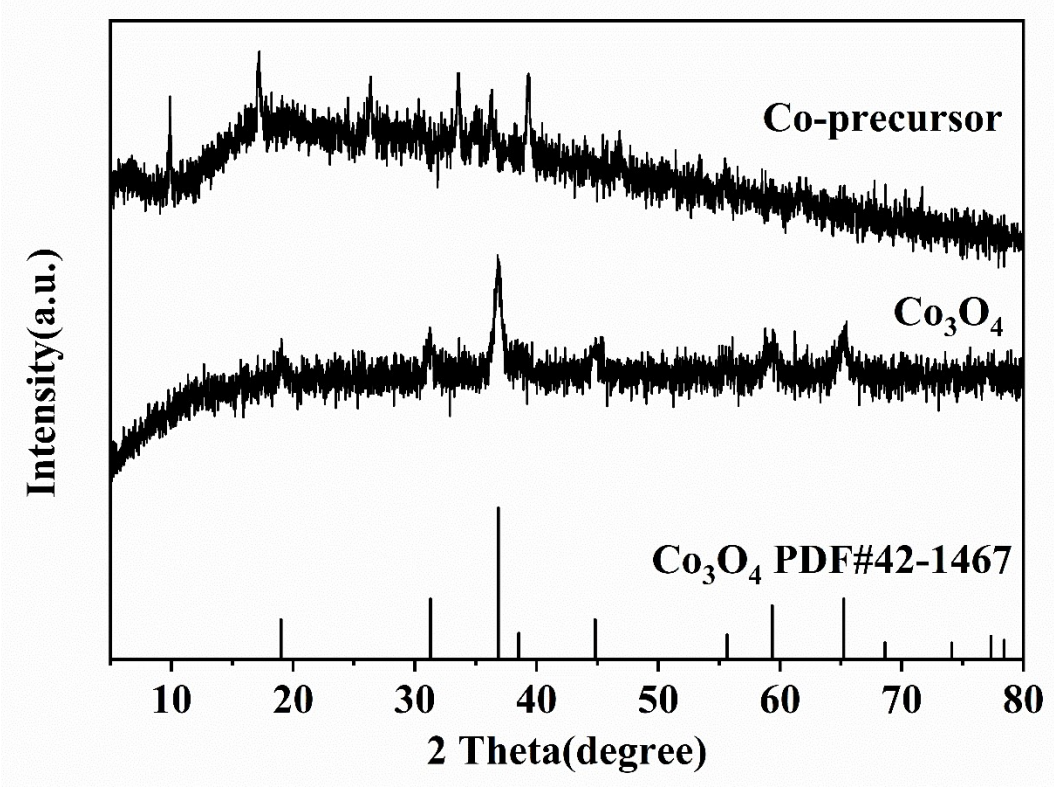

Fig. S2. XRD patterns of the precursors and pristine Co_3O_4 after hydrothermal without adding ammonium fluoride.

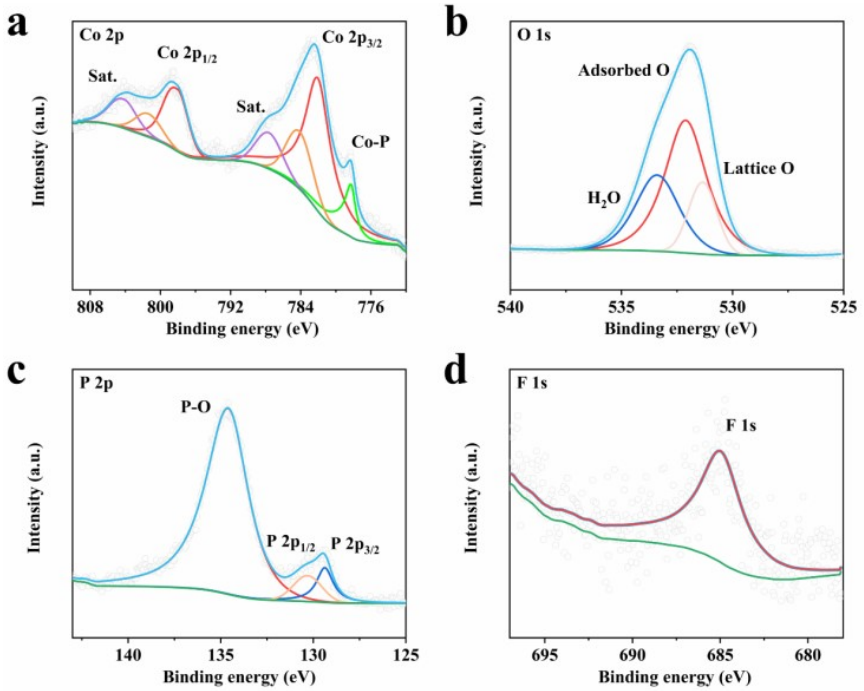

Fig. S3. The high resolution XPS spectra of F-P-Co_3O_4/NF, (a) Co 2p, (b) O 1s, (c) P 2p and (d) F 1s.

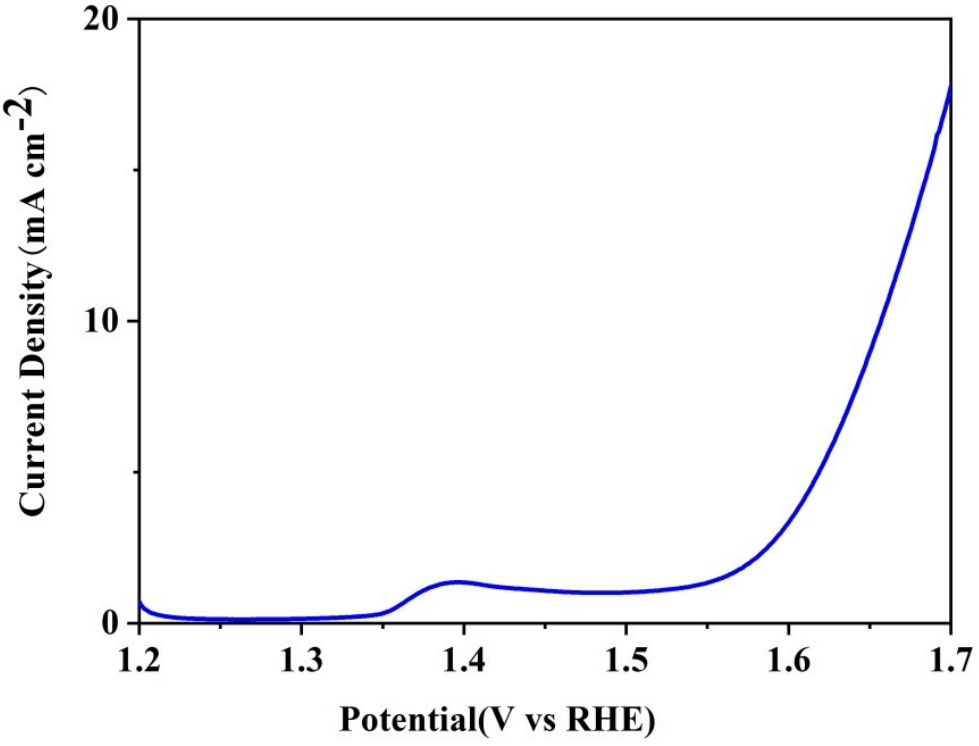

Fig. S4 Polarization curve of the Ni foam for OER with a scan rate of 5 mV s^{-1} in 1 M KOH.

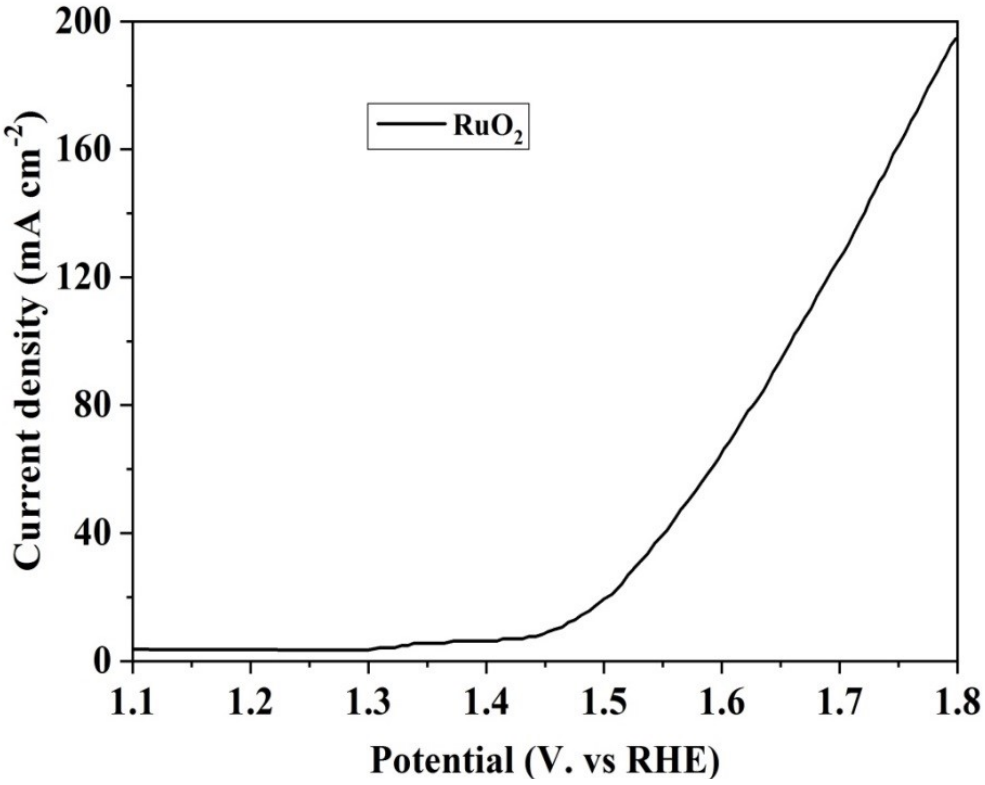

Fig. S5 Polarization curve of the RuO_2 for OER with a scan rate of 5 mV s^{-1} in 1 M KOH.

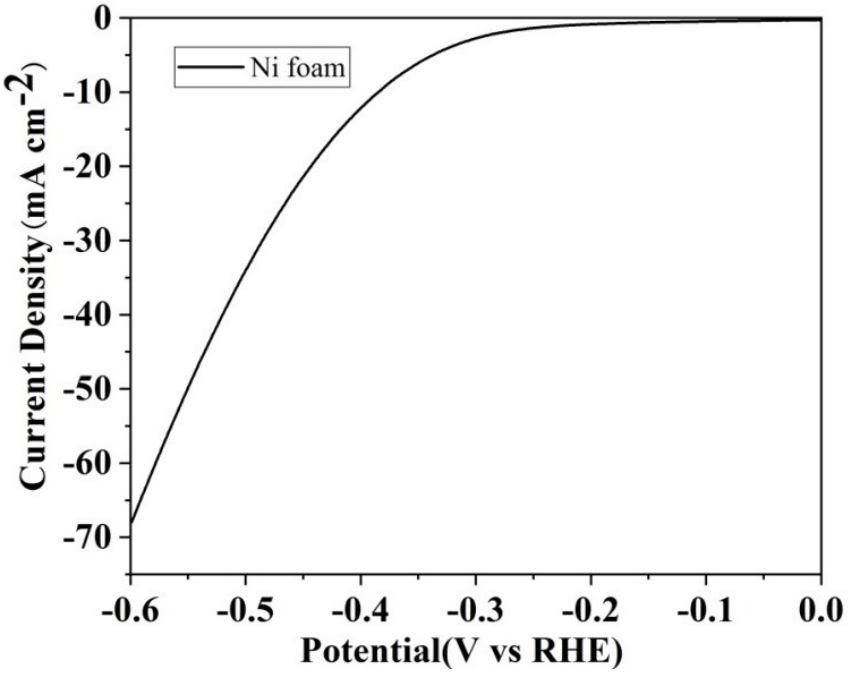

Fig. S6 Polarization curves of NF in 1.0 M KOH at a potential sweep rate of 5 mV s^{-1}.

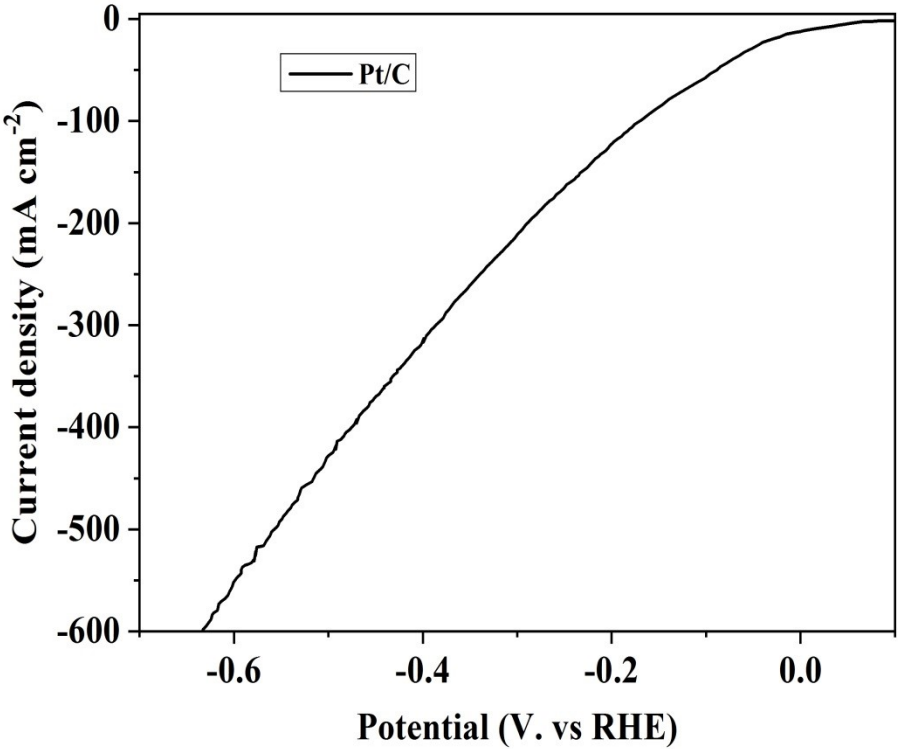

Fig. S7 Polarization curve of the Pt/C for HER with a scan rate of 5 mV s^{-1} in 1 M KOH.

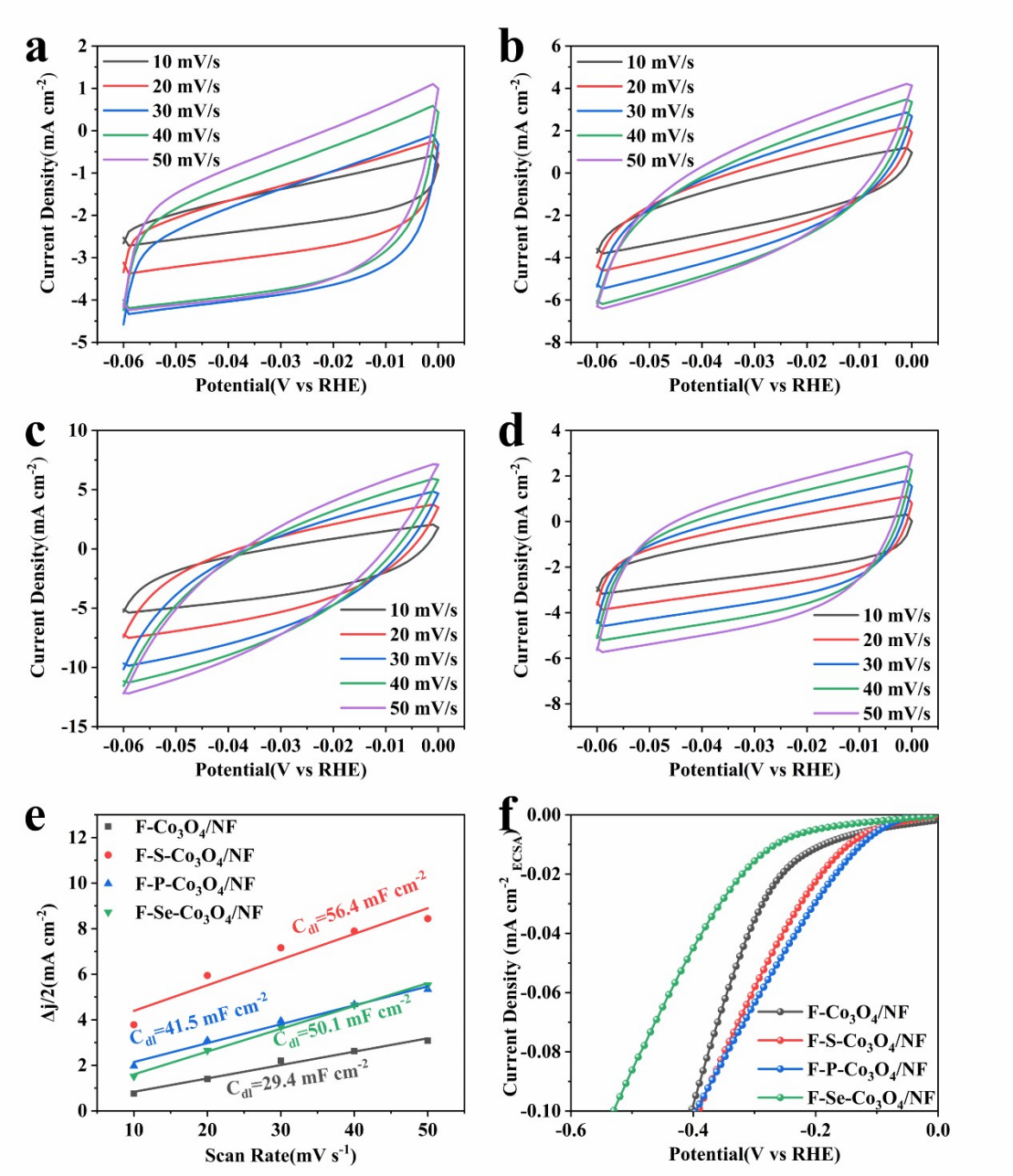

Fig. S8 CV curves of (a) F-Co_3O_4/NF, (b) F-S-Co_3O_4/NF, (c) F-P-Co_3O_4/NF and (d) F-Se-Co_3O_4/NF. (e) The C_{dl} linear fitting and calculations derived from CV of different sweep speeds. (f) The LSV curves normalized to the ECSA.

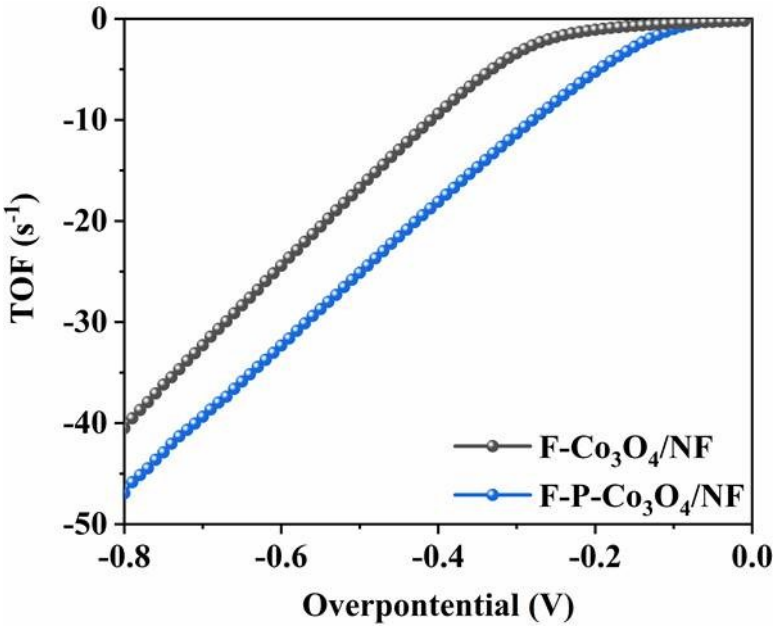

Fig. S9 TOF curves of F-Co_3O_4/NF and F-P-Co_3O_4/NF.

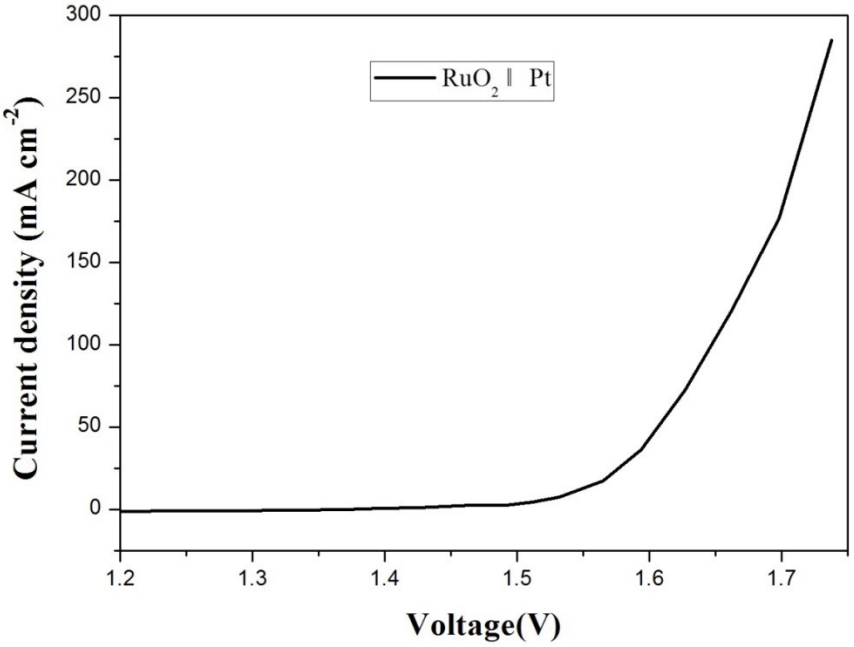

Fig. S10 Polarization curve of the RuO_2 and Pt for water splitting with a scan rate of 5 mV s^{-1} in 1 M KOH.

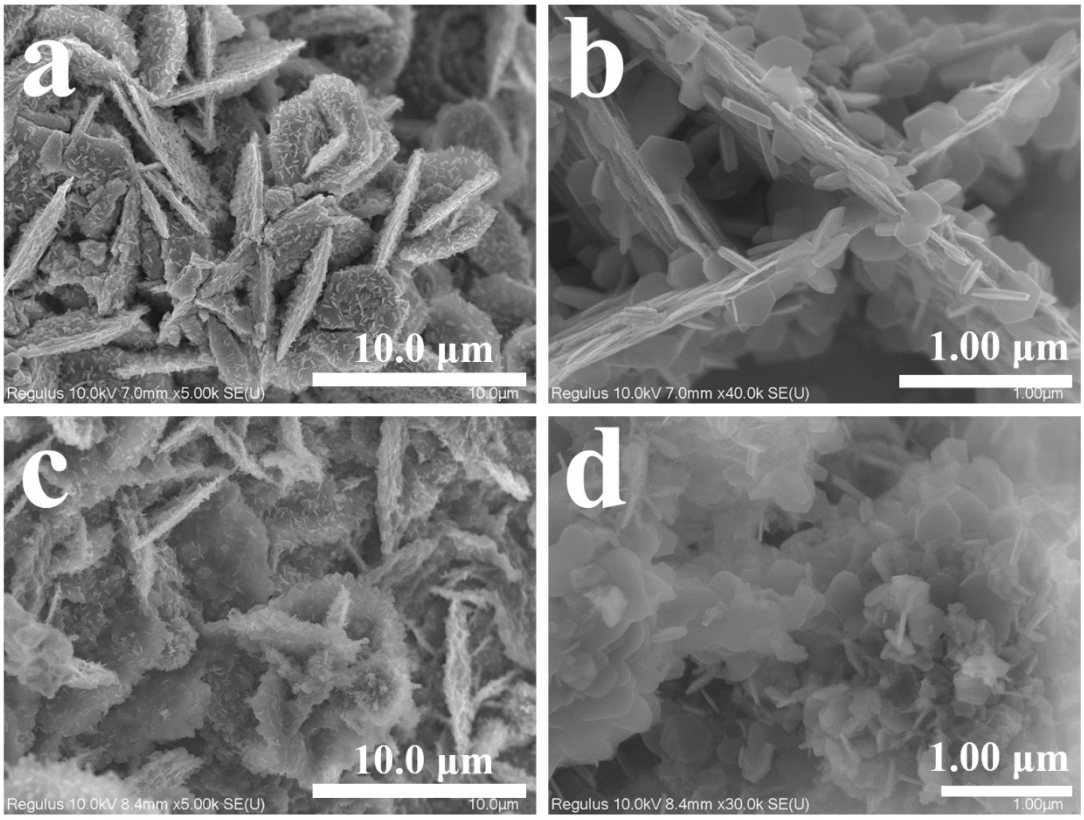

Fig. S11. Surface morphology of cathode (a,b) and anode (c,d) catalysts recovered by chronocurrent method for 15h.

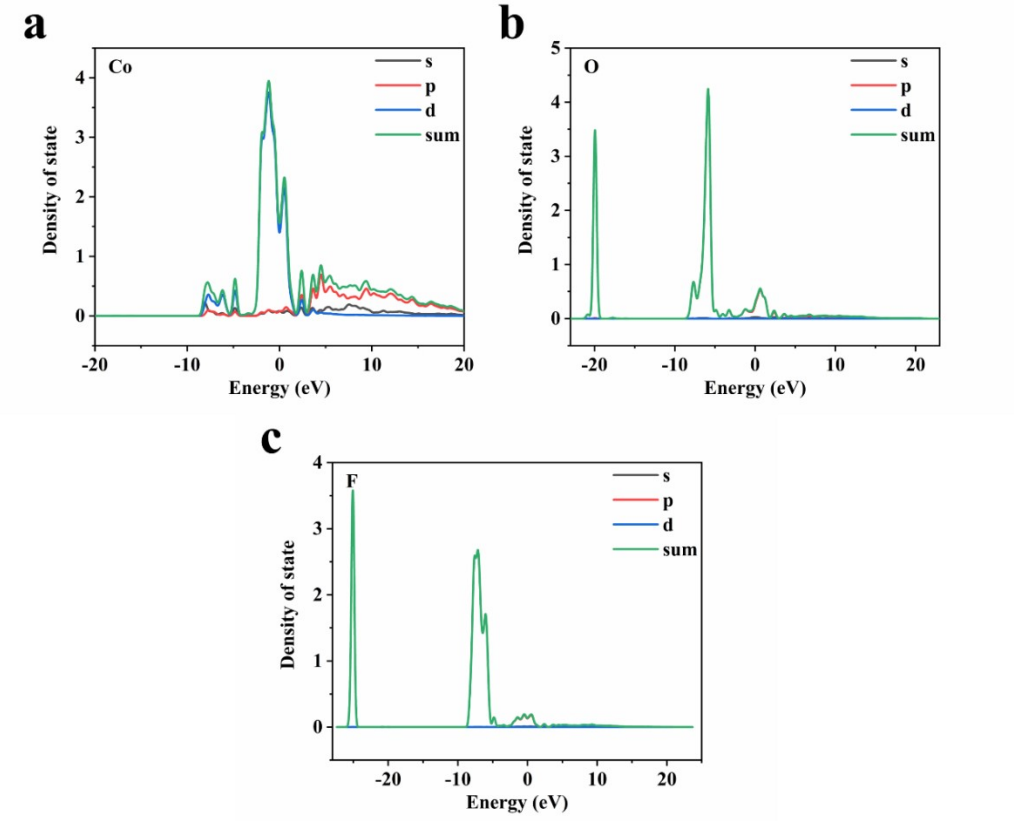

Fig. S12. Density of states for F-Co_3O_4, (a) Co, (b) O and (c) F.

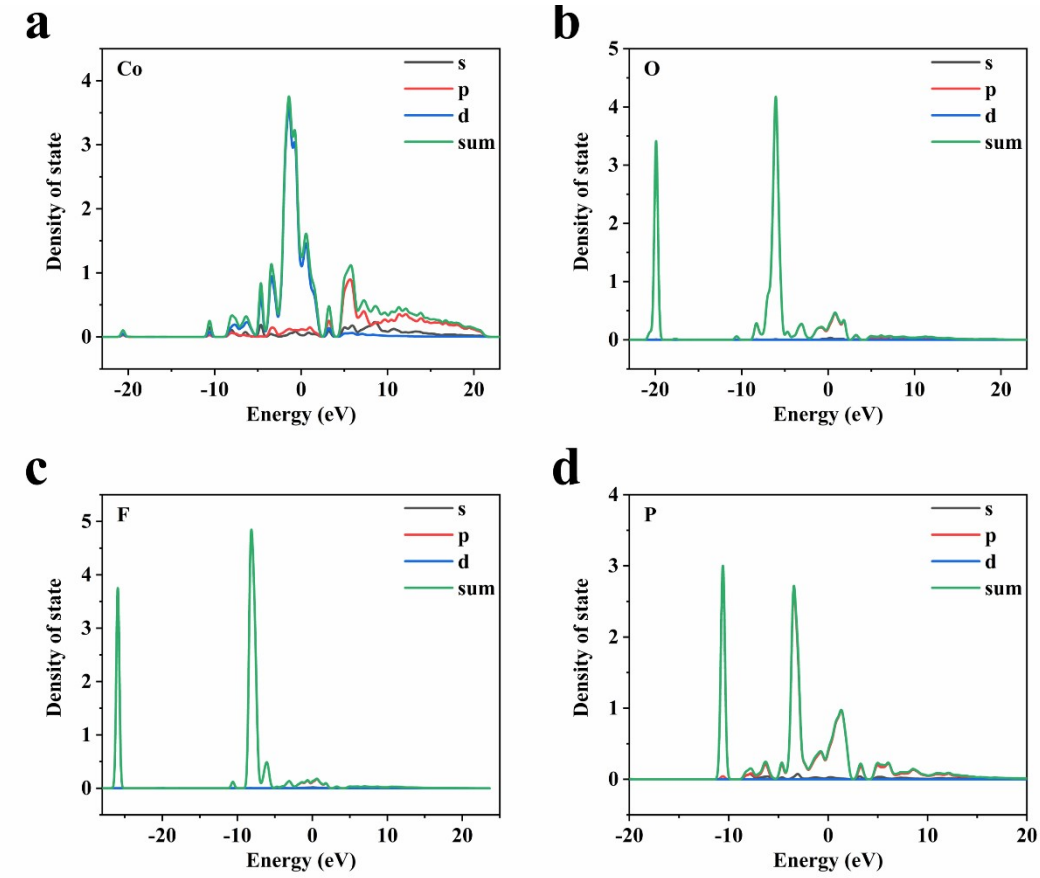

Fig. S13. Density of states for F-P-Co_3O_4, (a) Co, (b) O, (c) F and (d) P.

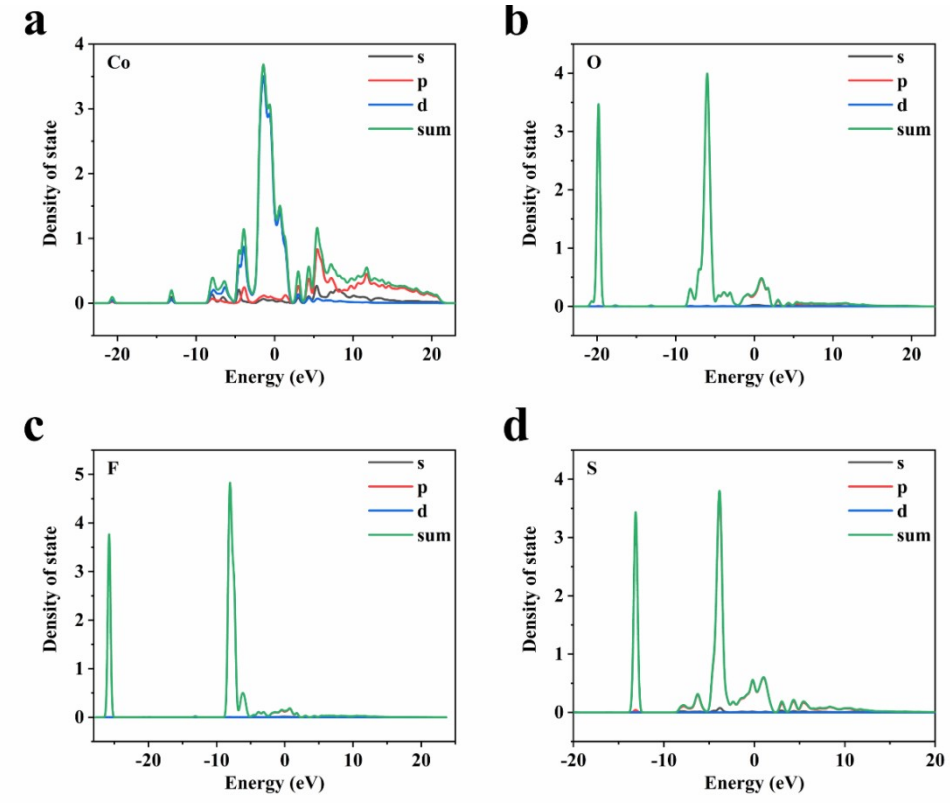

Fig. S14. Density of states for F-S-Co_3O_4, (a) Co, (b) O, (c) F and (d) S.

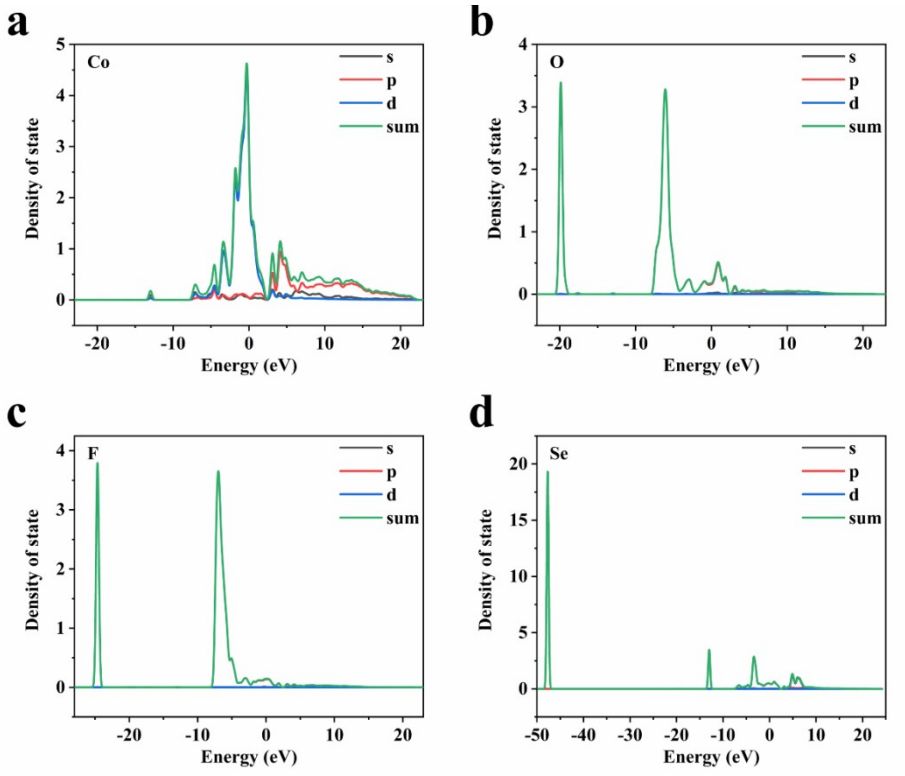

Fig. S15. Density of states for F-Se-Co_3O_4, (a) Co, (b) O, (c) F and (d) Se.

Table S1. OER performances of F-P-Co_3O_4/NF and other reported electrocatalysts in alkaline media.

Electrocatalyst	Electrolyte	Potential (mV) at 10 mA/cm^2	Tafel (mV/dec)	Ref.
F-P-Co_3O_4/NF	1 M KOH	192	32.1	This work
FeS/Ni_3S_2@NF	1 M KOH	192	70	1
NiFe LDH@NiCoP/NF	1 M KOH	220	48.6	2
Co/CoP@HOMC	1 M KOH	260	151	3
1D-Cu@Co-CoO/Rh	1 M KOH	260	99.7	4
Fe_2O_3/FeP	1 M KOH	264	47	5
p-NFNR@Ni–Co–P	1 M KOH	272	62	6
Fe-CoNiP	1 M KOH	280	99.1	7
CoFe@NC/NCHNSs-700	1 M KOH	285	39	8
Co_1-Fe_1-B-P	1 M KOH	294	49.5	9
$NiCo_2O_4$@$NiCo(OH)_2$/PNCF	1 M KOH	349	99.2	10

Table S2. HER performances of F-P-Co_3O_4/NF and other reported electrocatalysts in alkaline media.

Electrocatalyst	Electrolyte	Potential (mV) at 10 mA/cm^2	Tafel (mV/dec)	Ref.
F-P-Co_3O_4/NF	1 M KOH	110	79.9	This work
Fe-CoNiP	1 M KOH	110	90.6	7
NiFe LDH@NiCoP/NF	1 M KOH	120	88.2	2
CoFe@NC/NCHNSs-700	1 M KOH	120	144	8
Co/CoP@HOMC	1 M KOH	120	78	3
$NiCo_2O_4$@$NiCo(OH)_2$/PNCF	1 M KOH	121	83.2	10
p-NFNR@Ni–Co–P	1 M KOH	125	85	6
FeS/Ni_3S_2@NF	1 M KOH	130	124	1
1D-Cu@Co-CoO/Rh	1 M KOH	137	52.4	4
CoFeN-NCNTs//CCM	1 M KOH	151	130	11
H–Fe–CoMoS	1 M KOH	138	98	12

Table S3. Overall water splitting performances of F-P-Co_3O_4/NF and other reported electrocatalysts in alkaline media.

Electrocatalyst	Electrolyte	Potential (V) at 10 mA/cm^2	Ref.
F-P-Co_3O_4/NF(+/-)	1 M KOH	1.53	This work
Co/CoP@HOMC(+/-)	1 M KOH	1.54	3
Ni_3Se_2@FeOOH(+/-)	1 M KOH	1.54	13
Act-CoOOH/$W_{18}O_{49}$/NF(+/-)	1 M KOH	1.55	14
NiFe LDH@NiCoP/NF(+/-)	1 M KOH	1.57	2
P, Cu-$Co_{0.85}$Se/NF(+/-)	1 M KOH	1.57	15
Co_9S_8@NiFe-LDH HAs/NF(+/-)	1 M KOH	1.58	16
Ni-Fe-Co@CNSs(+/-)	1 M KOH	1.59	17
1D-Cu@Co-CoO/Rh(+/-)	1 M KOH	1.6	4
NiCoP/CoFeP@NF-12(+/-)	1 M KOH	1.61	18
p-NFNR@Ni–Co–P(+/-)	1 M KOH	1.62	6
Fe-CoNiP(+/-)	1 M KOH	1.62	7
Fe, Rh-Ni_2P/NF(+/-)	1 M KOH	1.62	19
CoNiP/NF(+/-)	1 M KOH	1.62	20
CoFe@NC/NCHNSs-700(+/-)	1 M KOH	1.66	8
$NiCo_2O_4$@$NiCo(OH)_2$/PNCF(+/-)	1 M KOH	1.66	10

Reference

1. H. Li, S. Yang, W. Wei, M. Zhang, Z. Jiang, Z. Yan and J. Xie, *J. Colloid Interface Sci.*, 2022, **608**, 536-548.
2. H. Zhang, X. Li, A. Hähnel, V. Naumann, C. Lin, S. Azimi, S. L. Schweizer, A. W. Maijenburg and R. B. Wehrspohn, *Adv. Funct. Mater.*, 2018, **28**, 1706847.
3. W. Li, J. Liu, P. Guo, H. Li, B. Fei, Y. Guo, H. Pan, D. Sun, F. Fang and R. Wu, *Adv. Energy Mater.*, 2021, **11**, 2102134.
4. P. K. L. Tran, D. T. Tran, D. Malhotra, S. Prabhakaran, D. H. Kim, N. H. Kim and J. H. Lee, *Small*, 2021, DOI: 10.1002/smll.202103826.
5. I. Ahmad, J. Ahmed, S. Batool, M. N. Zafar, A. Hanif, Zahidullah, M. F. Nazar, A. Ul-Hamid, U. Jabeen, A. Dahshan, M. Idrees and S. A. Shehzadi, *J. Alloy. Compd.*, 2022, **894**, 162409.

6. Y. Feng, R. Wang, P. Dong, X. Wang, W. Feng, J. Chen, L. Cao, L. Feng, C. He and J. Huang, *ACS Appl. Mater. Interfaces*, 2021, **13**, 48949-48961.
7. M. Ramadoss, Y. Chen, X. Chen, Z. Su, M. Karpuraranjith, D. Yang, M. A. Pandit and K. Muralidharan, *J. Phys. Chem. C*, 2021, **125**, 20972-20979.
8. S. Wang, H. Wang, C. Huang, P. Ye, X. Luo, J. Ning, Y. Zhong and Y. Hu, *Appl. Catal., B*, 2021, **298**, 120512.
9. X. Liu, G. He, H. Liu, Y. Zhu, J. Xiao and L. Han, *J. Alloy. Compd.*, 2022, **893**, 162208.
10. G. Chen, D. Chen, J. Huang, C. Zhang, W. Chen, T. Li, B. Huang, T. Shao, J. Li and K. K. Ostrikov, *ACS Appl. Mater. Interfaces*, 2021, **13**, 45566-45577.
11. G. Zhou, G. Liu, X. Liu, Q. Yu, H. Mao, Z. Xiao and L. Wang, *Adv. Funct. Mater.*, 2021, DOI: 10.1002/adfm.202107608.
12. Y. Guo, X. Zhou, J. Tang, S. Tanaka, Y. V. Kaneti, J. Na, B. Jiang, Y. Yamauchi, Y. Bando and Y. Sugahara, *Nano Energy*, 2020, **75**, 104913.
13. J. Gao, H. Ma, L. Zhang, X. Luo and L. Yu, *J. Alloy. Compd.*, 2022, **893**, 162244.
14. G. Hai, J. Huang, L. Cao, K. Kajiyoshi, L. Wang and L. Feng, *Appl. Surf. Sci.*, 2021, **564**, 150414.
15. Y. Wang, S. Li, D. Zhang, F. Tan, L. Li and G. Hu, *J. Alloy. Compd.*, 2021, **889**, 161696.
16. Y. Lu, C. Liu, Y. Xing, Q. Xu, A. M. S. Hossain, D. Jiang, D. Li and J. Zhu, *J. Colloid Interface Sci.*, 2021, **604**, 680-690.
17. W. Yaseen, N. Ullah, M. Xie, B. A. Yusuf, Y. Xu, C. Tong and J. Xie, *Surfaces and Interfaces*, 2021, **26**, 101361.
18. T. He, Y. He, H. Li, X. Yin, J. Ma, H. Shi, L. Zhou and L. Chen, *Int. J. Hydrogen Energy*, 2021, **46**, 37872-37883.
19. M. Chen, J. Duan, J. Feng, L. Mei, Y. Jiao, L. Zhang and A. Wang, *J. Colloid Interface Sci.*, 2022, **605**, 888-896.
20. H. Liu, R. Huang, W. Chen, Y. Zhang, M. Wang, Y. Hu, Y. Zhou and Y. Song, *Appl. Surf. Sci.*, 2021, **569**, 150762.